



BRNO UNIVERSITY OF TECHNOLOGY

VYSOKÉ UČENÍ TECHNICKÉ V BRNĚ

FACULTY OF ELECTRICAL ENGINEERING AND COMMUNICATION

FAKULTA ELEKTROTECHNIKY
A KOMUNIKAČNÍCH TECHNOLOGIÍ

DEPARTMENT OF FOREIGN LANGUAGES

ÚSTAV JAZYKŮ

MODERN IMAGING TECHNIQUES IN MEDICINE

MODERNÍ ZOBRAZOVACÍ METODY V MEDICÍNĚ

BACHELOR'S THESIS

BAKALÁŘSKÁ PRÁCE

AUTHOR

AUTOR PRÁCE

Aleš Pařízek

SUPERVISOR

VEDOUCÍ PRÁCE

Mgr. Šárka Rujbrová

BRNO 2016



Bakalářská práce

bakalářský studijní obor **Angličtina v elektrotechnice a informatice**

Ústav jazyků

Student: Aleš Pařízek

ID: 167670

Ročník: 3

Akademický rok: 2015/16

NÁZEV TÉMATU:

Moderní zobrazovací metody v medicíně

POKYNY PRO VYPRACOVÁNÍ:

Popište a srovnajte různé typy zobrazovacích metod, které se používají v moderní medicíně. Uveďte, jaké jsou jejich výhody a nevýhody. Proveďte závěrečné shrnutí.

DOPORUČENÁ LITERATURA:

[1] ZANG-HEE CHO. Foundations of Medical Imaging. John Wiley and Sons. Inc., 1993

[2] DRASTICH, A. Medical Imaging Systems: X-Ray, Computed Tomography, Magnetic Resonance Imaging. Brno: University of Technology Brno, 2000

[3] AUGUSTYNEK, M., ADAMEC, O., PENHAKER, M. Přístrojová zdravotnická technika I. Ostrava: VŠB - Technická univerzita Ostrava, 2010

[4] AUGUSTYNEK, M. Přístrojová zdravotnická technika II. Ostrava: VŠB - Technická univerzita Ostrava, 2011

Termín zadání: 11.2.2016

Termín odevzdání: 27.5.2016

Vedoucí práce: Mgr. Šárka Rujbrová

Konzultant bakalářské práce:

doc. PhDr. Milena Krhutová, Ph.D., předseda oborové rady

UPOZORNĚNÍ:

Autor bakalářské práce nesmí při vytváření bakalářské práce porušit autorská práva třetích osob, zejména nesmí zasahovat nedovoleným způsobem do cizích autorských práv osobnostních a musí si být plně vědom následků porušení ustanovení § 11 a následujících autorského zákona č. 121/2000 Sb., včetně možných trestněprávních důsledků vyplývajících z ustanovení části druhé, hlavy VI. díl 4 Trestního zákoníku č.40/2009 Sb.

ABSTRAKT

Cílem této práce je popsat základní principy a fyzikální veličiny spjaté s jednotlivými zobrazovacími metodami a poté jednotlivé metody porovnat. Práce popisuje vznik rentgenového záření, jeho interakci s různými materiály a metody snímání pro vytvoření obrazů. Dále se práce zabývá základním principem vytvoření 3D obrazů pomocí počítačové tomografie a jednotlivými generacemi tomografických strojů. V poslední části se práce věnuje principu nukleární magnetické resonance a základním parametrům pro vytvoření obrazů pomocí MRI systémů.

KLÍČOVÁ SLOVA

Rentgenové záření, elektromagnetické záření, radiografie, mamografie, rentgenka, rozlišení, kontrast, tomografie, skiografie, skiaskopie, proton, nukleární magnetická rezonance, magnetické pole

ABSTRACT

The aim of this work is to describe physical phenomena and basic principles relevant to individual imaging methods and to compare them. The bachelor thesis describes generation of x-rays, interaction of x-rays with various media and methods of detecting the x-rays. In addition, the work describes basic principles of creating 3D images using computed tomography and individual generations of CT machines. Lastly, the work aims on the principle of nuclear magnetic resonance and basic parameters for creation of MRI images.

KEYWORDS

X-rays, electromagnetic radiation, radiography, mammography, x-ray tube, resolution, contrast, tomography, skiagraphy, fluoroscopy, proton, nuclear magnetic resonance, magnetic field

PAŘÍZEK, A. *Moderní zobrazovací metody v medicíně*. Brno: Vysoké učení technické v Brně, Fakulta elektrotechniky a komunikačních technologií, 2016. 43 s., Vedoucí práce: Mgr. Šárka Rujbrová

PROHLÁŠENÍ

Prohlašuji, že svou bakalářskou práci na téma Moderní zobrazovací metody v medicíně jsem vypracoval samostatně pod vedením vedoucího bakalářské práce a s použitím odborné literatury a dalších informačních zdrojů, které jsou všechny citovány v práci a uvedeny v seznamu literatury na konci práce.

Jako autor uvedené bakalářské práce dále prohlašuji, že v souvislosti s vytvořením této bakalářské práce jsem neporušil autorská práva třetích osob, zejména jsem nezasáhl nedovoleným způsobem do cizích autorských práv osobnostních a/nebo majetkových a jsem si plně vědom následků porušení ustanovení § 11 a následujících zákona č. 121/2000 Sb., o právu autorském, o právech souvisejících s právem autorským a o změně některých zákonů (autorský zákon), ve znění pozdějších předpisů, včetně možných trestněprávních důsledků vyplývajících z ustanovení části druhé, hlavy VI. díl 4 Trestního zákoníku č. 40/2009 Sb.

V Brně dne

.....

(podpis autora)

PODĚKOVÁNÍ

Děkuji vedoucí bakalářské práce Mgr. Šárce Rujbrové a odbornému konzultantovi Ing. Martinu Mézlovi za účinnou metodickou, pedagogickou a odbornou pomoc a další cenné rady při zpracování mé bakalářské práce.

V Brně dne

.....

(podpis autora)

CONTENTS

LIST OF FIGURES	1
LIST OF TABLES	2
1 INTRODUCTION	3
2 X-RAY IMAGING	5
2.1 GENERAL DIVISION OF X-RAY IMAGING SYSTEMS	5
2.2 THE HISTORY OF X-RAY IMAGING	7
2.3 BASIC PRINCIPLE OF CREATING AN IMAGE.....	7
2.4 PROPERTIES OF X-RAYS	8
2.5 GENERATION OF X-RAYS	9
2.6 X-RAY INTERACTION WITH MATTER	12
2.7 DETECTION OF X-RAYS	14
2.8 ELECTRONICS IN X-RAY IMAGING SYSTEMS	16
2.9 COLOR X-RAY IMAGING.....	16
3 COMPUTER TOMOGRAPHY.....	18
3.1 BASIC CT PRINCIPLE.....	18
3.2 GENERATIONS OF CT SCANNERS.....	19
3.3 SLIP RING TECHNOLOGY AND HELICAL SCANNING	21
3.4 MULTI-SLICE CT SYSTEMS.....	23
4 MAGNETIC RESONANCE IMAGING	25
4.1 THE HISTORY OF MAGNETIC RESONANCE IMAGING	25
4.2 NUCLEAR MAGNETIC RESONANCE.....	26
4.2.1 QUANTUM MODEL - PARALLEL AND ANTIPARALLEL PROTONS.....	27
4.2.2 CLASSICAL MODEL - PRECESSION MOTION AND LARMOR FREQUENCY	28
4.2.3 QUANTUM MODEL OF MAGNETIC RESONANCE.....	29
4.2.4 CLASSICAL MODEL OF MAGNETIC RESONANCE.....	30

4.2.5	FREE INDUCTION DECAY (FID) SIGNAL	32
4.3	BASIC MEASUREMENT TECHNIQUES.....	33
4.4	SPATIAL LOCALIZATION.....	33
4.5	MRI SYSTEM	35
5	CONCLUSION.....	37
	BIBLIOGRAPHY	39
	APPENDIX.....	40

LIST OF FIGURES

Figure 1 – Simple representation of mammography and radiography (taken from [2])...	5
Figure 2 – Simple representation of fluoroscopy (taken from [2]).....	6
Figure 3 – Simple representation of digital detection of x-rays (taken from [2]).....	6
Figure 4 – Electromagnetic spectrum. Retrieved May 17, 2016 from http://www.cyberphysics.co.uk/topics/light/emspect.htm	9
Figure 5 – Block schematic of general x-ray (taken from [2])	10
Figure 6 – X-ray tube with static anode (taken from [2]).....	11
Figure 7 – Representation of X-ray intensity frequency characteristics (taken from [2])	12
Figure 8 – Illustration of Compton scattering (taken from [2]).....	14
Figure 9 – Illustration of CT scanning process (taken from [2])	19
Figure 10 – Illustration of typical CT system (taken from [2])	20
Figure 11 – Slip ring in CT scanner. Retrieved May 17, 2016 from http://www.wikiradiography.net/page/Slip+Rings).....	22
Figure 12 – A) Planar scans of conventional CT system B) Helical scanning. Retrieved May 17, 2016 from http://imaging.cancer.gov/patientsandproviders/cancerimaging/ctscans	23
Figure 13 – Illustration of cone beam artifact for different pitch values. Retrieved May 17, 2016 from http://www.slideshare.net/VivekElangovan1/ctdi-42682868	24
Figure 14 – Precession of a single proton around the magnetic field (taken from [2])..	29
Figure 15 – Simultaneous precession of vector M around the vectors B0 and B1 (taken from [2]).....	32
Figure 16 – Pair of gradient coils used for localization on the y-axis (taken from [2]) .	34
Figure 17 – Individual processes of spatial localization (taken from [2])	35
Figure 18 – Typical MRI system configuration (taken from [2]).....	36
Figure 19 – Comparison between axial view of CT scan and several MRI scans. Retrieved May 3, 2016 from https://www.youtube.com/watch?v=sz0qd5q6FDU	42
Figure 20 – Typical x-ray scan. Retrieved May 3, 2016 from http://med.fau.edu/research/focus.php	43

LIST OF TABLES

Table 1 – The history of MRI	40
Table 2 – Elements of interest for MRI	41
Table 3 – Comparison of individual imaging modalities	43

1 INTRODUCTION

In my bachelor thesis, I deal with imaging technology and systems used in medicine with a special focus on x-ray imaging, Computer Tomography (CT) and Magnetic Resonance Imaging (MRI). Imaging systems are a very important instrument for determining a diagnosis of a patient. While there are many tests or measurements which can say a lot about a health condition of a patient by providing results in numbers or other means, there are also symptoms which require being displayed in visible pictures to be diagnosed properly. This can be a very difficult task as every intervention in the human body is likely to be problematic. Therefore, development of imaging technology in medicine is directed towards the safety of the patient and personnel who operates it, while providing reasonable results for determining appropriate therapy.

In my thesis, I deal with various specific imaging systems, from the simplest x-ray systems like radiographs or mammographs to very complex systems like CT or MRI. I describe the principle of their function, the history of their development, the possibility to be harmful to human body, the prevention of hazards and specific areas of medicine in which they are used. My thesis is mainly focused on technical and scientific point of view of imaging technology and thus, I will focus mainly on the problems with construction of specific devices and their effectivity in providing readable results.

The most known and used imaging system in medicine is x-ray imaging. I describe x-ray systems in detail as it also provides a good starting point for describing a more complex system that is based on x-ray imaging – Computer Tomography.

Computer tomography is one of the major topics of my work. This system is based on relatively simple principles which are, however, problematic to realize. I focus mainly on how to utilize the phenomena from the traditional x-ray imaging in 3D projection, computing methods to create 3D images and a construction of specific machines.

Another major topic of my thesis is magnetic resonance imaging. This imaging method is based on completely different physical phenomena than x-ray imaging systems but provides very similar results in comparison to CT. My thesis focuses on

describing the basic principle of MRI and comparison of MRI to CT as these two imaging methods are the most common means of obtaining 3D images of the human body.

There are many other imaging methods which also deserve to be mentioned – ultrasound, PET systems etc. Each of these methods has its place in modern medicine and is further developed. However, each of these methods is complex and based on principles which are mostly not similar to the methods I describe in the thesis. For the sake of having enough space for information about the methods I chose to describe in my thesis, I will not deal with these imaging systems.

The purpose of this work is to describe specific imaging methods used in medicine, to analyze their advantages and disadvantages and to make a comparison between them.

2 X-RAY IMAGING

X-ray imaging and its 3-dimensional equivalent (computer tomography) are well-known imaging systems used for more than 100 years since the discovery of x-rays in 1895 by Wilhelm Conrad Röntgen. X-rays are photons of high energy. Their generation in x-ray tubes creates beams of electromagnetic radiation. These beams pass differently through various media and therefore, x-ray imaging is based on through transmission and analysis of absorbed x-ray radiation.

2.1 GENERAL DIVISION OF X-RAY IMAGING SYSTEMS

Most commonly, the x-rays are detected by a combination of the phosphor screen and light-sensitive film (figure 1). This method is used for common techniques like the mammography and radiography as it provides good results in terms of image quality. However, these results are given in the analog form, which is not compatible with modern digital systems. These techniques are also generally called *skiagraphy* and are used to obtain a single static image.

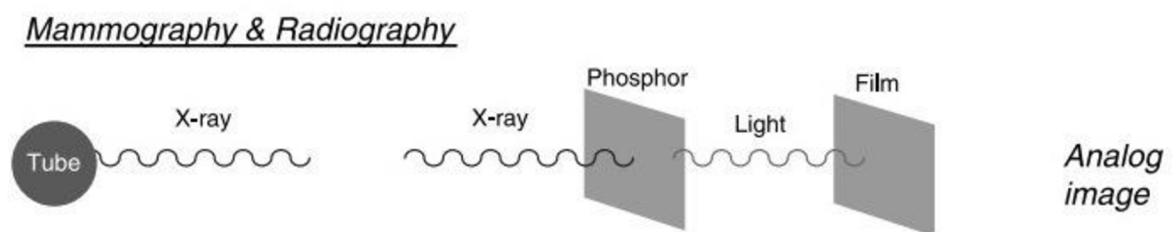


Figure 1 – Simple representation of mammography and radiography (taken from [2])

Variation of this system is *fluoroscopy* (figure 2). This method uses an electron intensifier to supply an image signal to CMOS camera, which then projects the image directly onto a TV screen. The results are, as in the case of mammography and radiography, given in the analog form. The results are a sequence of images – it is possible to analyze displayed objects in time. The most problematic disadvantage of this method is that there is noticeable image degradation due to several conversion steps from electrons to light.

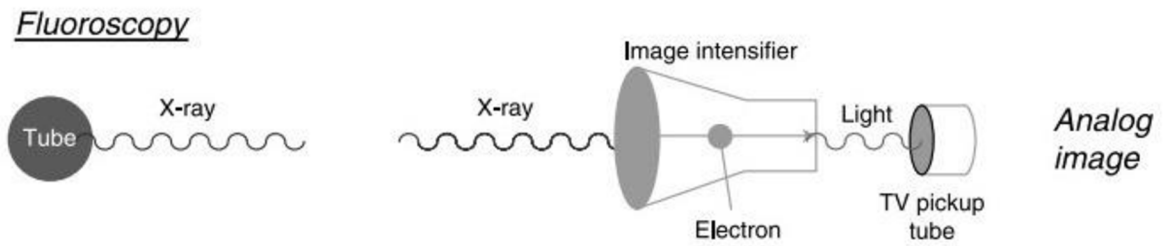


Figure 2 – Simple representation of fluoroscopy (taken from [2])

An alternative to these conventional systems uses a digital detector which converts x-ray radiation directly into the electrical signal of digital nature (figure 3). Using this method ensures lower operating cost and compatibility with modern digital systems. In my bachelor thesis, I will mainly focus on systems using digital detectors, as the conventional methods are starting to be outdated and are expected to be soon replaced with digital technology.

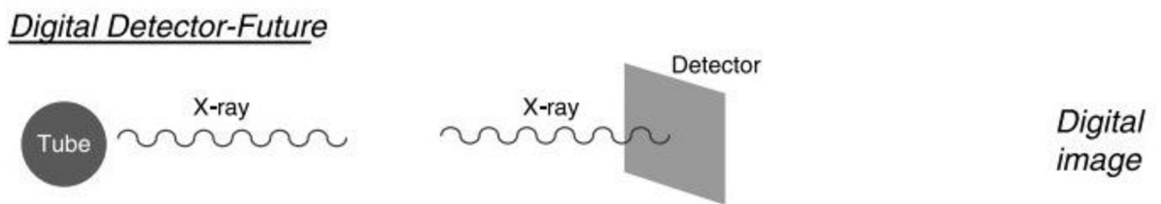


Figure 3 – Simple representation of digital detection of x-rays (taken from [2])

The operation of these x-ray scanners can be complicated but the principle behind x-ray imaging can be quite simply described. To work as an imaging modality, x-ray imaging needs a generator of x-rays, an object to be imaged, a detector of the radiation and a device to convert it to a visible image. In the case of modern imaging systems, the last step is dedicated to the ability to convert absorbed radiation to an electrical signal.

While commonly used and inexpensive, x-ray imaging has a number of serious limitations. There are difficulties with creating images for soft tissues in the human body as they have small attenuation coefficient (described in chapter 2.3 Principle of creating an image), which leads to images with low contrast. Another big issue is that 3-dimensional structures are displayed via 2-D images, which leads to reduced image contrast. Finally, resulting images from x-ray do not provide quantitative data and therefore require specialized training to assess given results. Luckily, many of these

limitations are solved by an extension to the traditional x-ray imaging – computed tomography (CT). Computed tomography generally uses principles of x-ray imaging to take many images of the object from various angles and then constructs a 3-D projection of this object. CT systems use much more computer power and are generally more complex in terms of construction. Chapter 3 of this work is dedicated to these systems.

2.2 THE HISTORY OF X-RAY IMAGING

X-rays were discovered by a German physicist Wilhelm Conrad Röntgen in 1895 by observation of fluorescence. While he is credited with the discovery of x-rays because he was the first who systematically studied them, many other scientists have observed fluorescence prior to him. The discovery of the x-rays was based on Crookes tubes – experimental tubes used for generation of energetic electron beams. Crookes tubes created free electrons by ionization of the residual air in the tube using high DC voltage (between several kilovolts to values as high as 100kV). This process accelerated electrons coming from the cathode to such a high velocity that their collision with anode radiated x-rays. Röntgen was the first who was interested in examining this phenomenon and he was the first person to receive the Nobel Prize for physics in 1901.

Röntgen was also the person who invented the name “x-rays,” however they were also referred to as Röntgen-rays. Different names for individual imaging methods are also associated with the name of Röntgen-rays, such as x-ray radiograms opposed to Röntgenograms, which are used even to this day in some languages (Czech, German).

Only a few years after the discovery, imaging machines based on x-rays began to be manufactured and sold. Today, x-ray and its 3-dimensional extension (computer tomography) are commonly known and used in medical diagnosis.

2.3 BASIC PRINCIPLE OF CREATING AN IMAGE

The whole process of creating an image is based on detecting an attenuation of x-rays passing through an object (a patient). As different materials cause a different level of attenuation of x-rays, an image corresponding to this property can be easily created. The attenuation characteristics are described by Beer-Lambert law (2.1):

$$I(z) = I_0 \cdot \exp(-\mu z) \quad (2.1)$$

Where $I(z)$ refers to x-ray intensity at a detector, I_0 refers to x-ray intensity at a generator, μ is the attenuation coefficient which is different for each material, and z is the distance between the detector and the generator of the x-rays. By determining a value of $I(z)$ for a set of individual detectors, we can obtain a set of attenuation values which then give a corresponding image.

With this in mind, we can say that x-ray imaging is especially good at providing good contrast between materials with a high attenuation coefficient and materials with low attenuation coefficient (hard and soft tissues in the human body) – for this reason, x-ray systems represent one of the first diagnostic methods used for determining bone fractures.

2.4 PROPERTIES OF X-RAYS

X-rays (X-radiation) is a form of electromagnetic radiation with a wavelength ranging from 0.01 to 10 nanometers – this corresponds to frequencies from $3 \cdot 10^{16}$ Hz to $3 \cdot 10^{19}$ Hz and photon energies from 100 eV to 100 KeV (electron-volts).

In figure 4, we can see the representation of the whole electromagnetic spectrum with approximate values of wavelength. With respect to the wavelength and photon energy of x-rays, we can further divide them to *hard* x-rays and *soft* x-rays. Generally, hard x-rays have a shorter wavelength and thus, higher values of frequency and energy. In terms of imaging systems, hard x-rays are mostly used in radiography as they have a better ability to pass through objects. Soft x-rays are used less commonly – mostly in mammography.

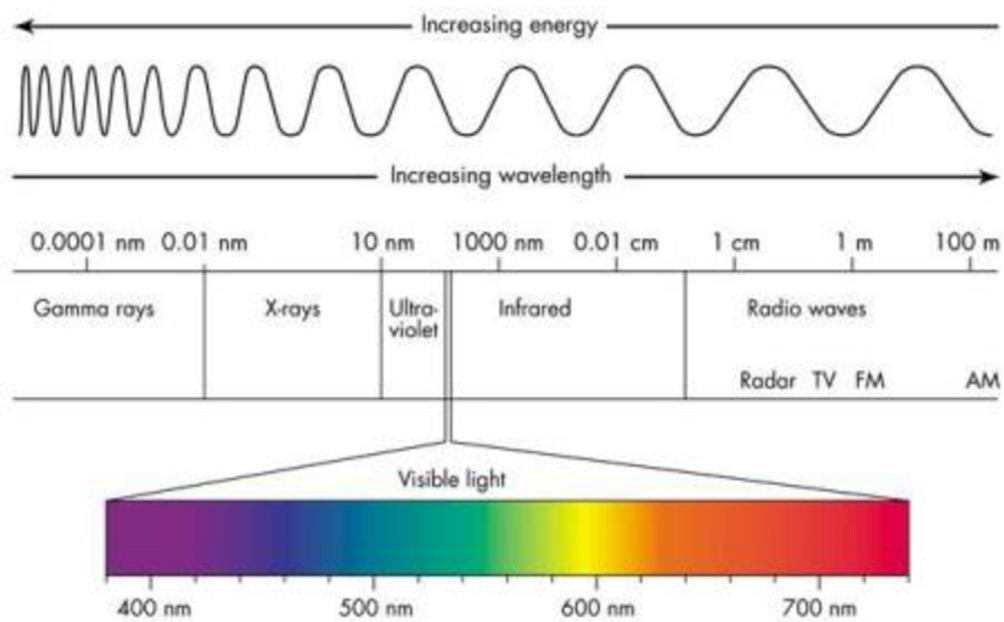


Figure 4 – Electromagnetic spectrum. Retrieved May 17, 2016 from <http://www.cyberphysics.co.uk/topics/light/emspect.htm>

X-rays represent ionizing radiation - with high enough doses (long exposure, or exposure to high energy radiation), there is a risk of tissue damage. *Absorbed dose* of radiation is represented by unit *rad* (non-SI) or *gray* (SI). The definition in SI units says that 1 rad causes 0.01 joule of energy to be absorbed per kilogram of matter; it can be also described as a dose that causes 100 ergs of energy ($1 \text{ erg} = 10^{-7} \text{ J}$) to be absorbed by one gram of matter. To describe the harmful effects on human body, the quantity called *dose equivalent* is used; this quantity uses SI unit called *sievert* (*Sv*). The dose of 50 *rads* causes radiation sickness - for a reference, a usual chest x-ray exposure is about 50 *millirads*, which is harmless supposing that the patient does not undergo this examination very often.

2.5 GENERATION OF X-RAYS

For the generation of x-rays, several types of x-ray tubes are used. In figure 6, we can see a typical x-ray tube. The principle of generating the x-rays is based on creating free electrons via heating a tungsten filament and then accelerating them via high anode voltage. The high-velocity electrons then collide with the anode, creating x-rays. Standard x-ray systems use transformers to generate high voltage needed for electron acceleration (figure 5). X-ray photon energy is proportional to applied acceleration

voltage. The voltage of 10kV will produce photons with energy of 10KeV. The total number of photons is then proportional to the cathode current, which has generally values of milliamperes.

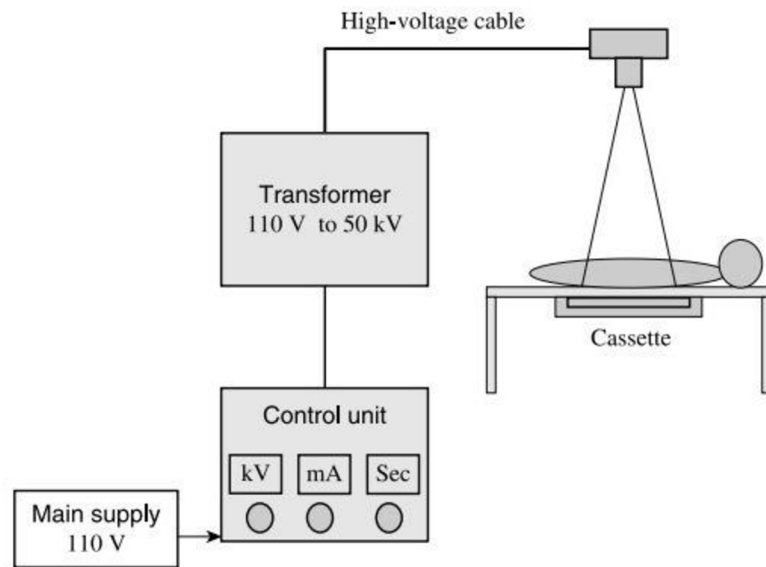


Figure 5 – Block schematic of general x-ray (taken from [2])

There are two types of x-ray tubes used in medical imaging systems today – x-ray tubes with a static anode and x-ray tubes with a rotational anode. Tubes with rotational anodes are the most common today, static anode tubes are mostly used in dental x-rays. As the electrons collide with the material of the anode, high amount of heat is produced – x-ray tubes have very low efficiency (only about 1%). Thus, it is important to reduce the produced heat. The rotational anode serves this purpose well as the target of accelerated atoms is constantly in motion and the heat is redistributed over bigger area. In computed tomography, there is usually a need for x-ray tubes with higher power to ensure shorter scan times. These x-ray tubes usually need additional means of cooling – most commonly cooling liquids. Furthermore, the inefficiency of generating x-rays does not end with heat problems. The x-rays are not collimated and the radiation is emitted in all possible directions. Therefore, only a small percentage of radiation reaches a detector.

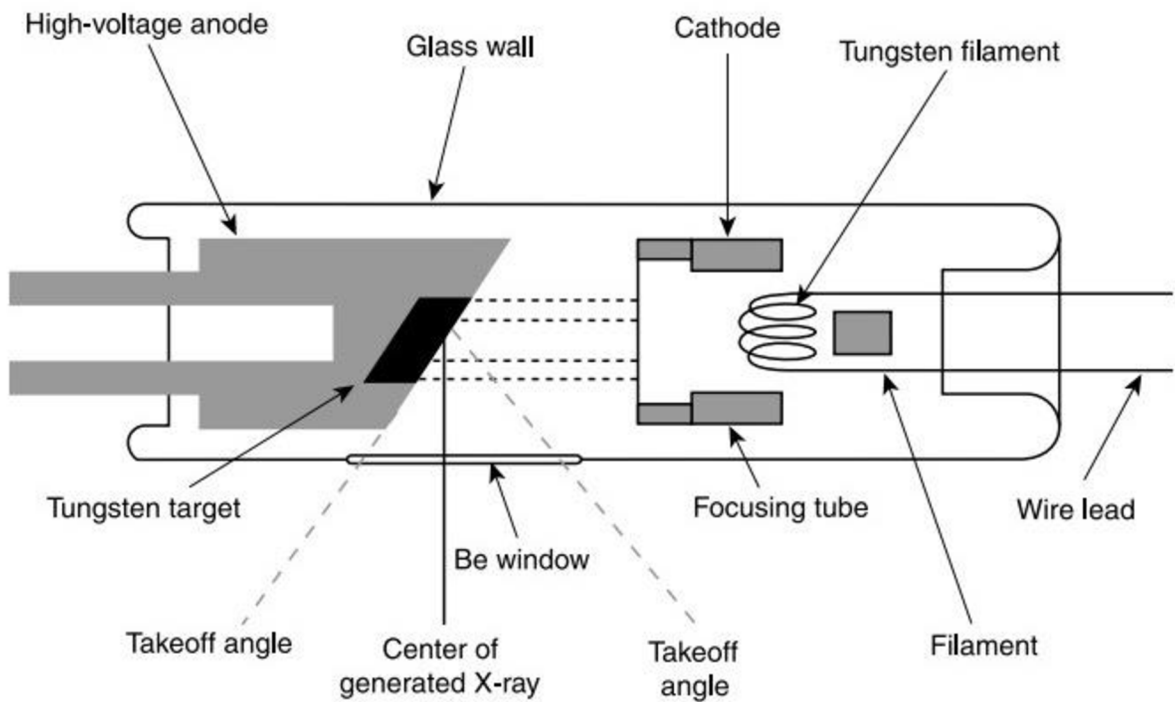


Figure 6 – X-ray tube with static anode (taken from [2])

There are two types of radiation created in x-ray tubes: *Bremsstrahlung* and so-called *characteristic radiation*. The word *Bremsstrahlung* has its origin in German language and is used to describe radiation which is created when the electrons are decelerated. The *Bremsstrahlung* radiation is generated by electrons which interact with the shells of atom nuclei – as the electrons hit the anode, they are scattered by the strong electric field near the nuclei with a high proton number. The characteristic property of *Bremsstrahlung* radiation is that it has a continuous spectrum (figure 7). With increasing intensity, the radiation shifts towards higher frequencies. The characteristic radiation, on the other hand, is created by electrons with high enough energy to knock an orbiting electron from the inner shell of a metal atom – as a result of this, electrons from outer shell fill up the vacancy and x-ray photons are produced. The characteristic radiation produces peaks of intensity (also known as spectral lines) at particular energy levels. The spectral lines generated depend on the material of the anode – thus the name characteristic radiation. In the real world, the radiation is filtered – intentionally or not (figure 7). The low-energy photons are completely attenuated, creating a high-pass filter response – as a result, the whole spectrum of emitted radiation has a band-type characteristic with several peaks on particular energy levels.

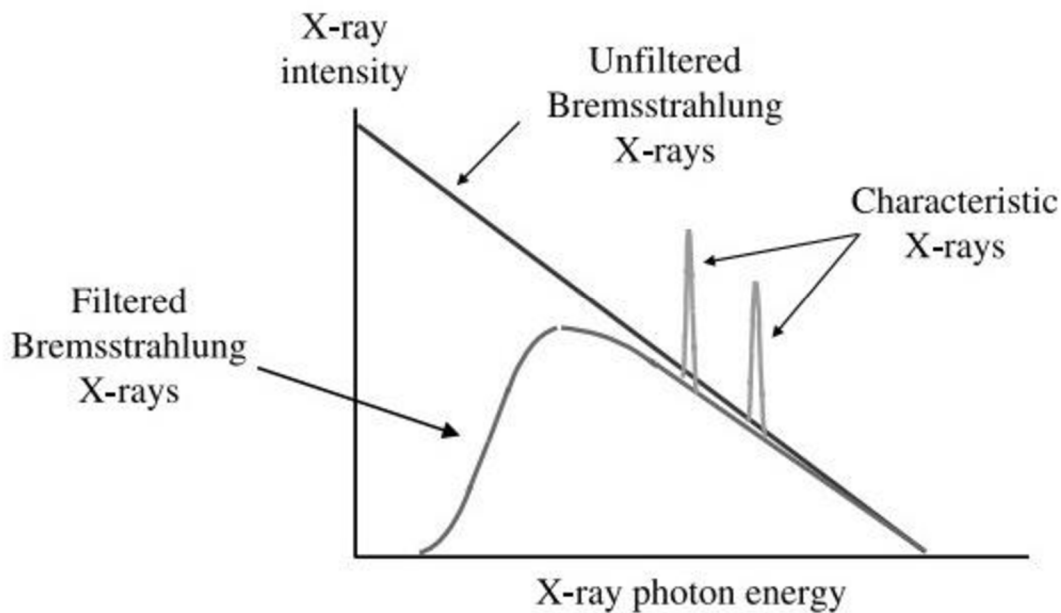


Figure 7 – Representation of x-ray intensity frequency characteristics (taken from [2])

2.6 X-RAY INTERACTION WITH MATTER

X-rays interact with matter in three most notable ways: photoelectric absorption, Compton scattering, and Rayleigh scattering. The strength of these interactions is mainly affected by the energy of x-rays and elemental composition of the material; the chemical properties of the material are mostly irrelevant here as the energy of x-ray photons is much higher than the chemical binding energies. For the soft x-rays and lower hard x-rays, photoelectric absorption is the dominant phenomenon, while scattering interactions are dominant for x-rays with higher energy. The photoelectric absorption is a process in which the photon energy is absorbed by the orbital electron in the atom – generally, this is the interaction which is the most useful for x-ray imaging. The Compton scattering effect is an interaction in which the photon gives a part of its energy to the electron and then travels on with less energy and altered direction. While this interaction can be utilized in some methods (Compton cameras), it is in most cases considered an undesirable phenomenon. In the case of Rayleigh scattering (also known as coherent scattering), the whole energy of photon interacts with the atom and is later radiated again in a random direction. As a result, the photon has the same amount of energy, but travels in a different direction, which is a completely undesired effect in x-ray imaging.

The photoelectric absorption is the event in which the emitted photon effectively disappears - the photon energy is completely absorbed by the orbital electron, which is then ejected from the atom, this process ionizes the atom to which the electron was bound and produces photoelectron which then travels in the same direction. This photoelectron has a high probability of causing ionization of additional atoms in its path. The vacancy in the shell is then filled with the electron from the outer shell or from atoms of surrounding environment. In the photoabsorption, the x-rays are therefore converted into electrical charges, which is essentially very useful for radiation detection. The probability of this interaction to happen can be simply calculated by formula Z^3/E^3 , where Z is the atomic number and E is the energy of the photon. However, this formula does not apply to close to inner shell electron binding energies as there are great changes in interaction probability.

The Rayleigh scattering describes the event in which the photons are scattered by the atom as a whole. It is often referred to as coherent scattering as the electrons bound to the atom interact coherently and there is no energy transferred to the material which the photon interacts with. The only result of this interaction is that the photon changes its direction. It is generally an undesired effect as it negatively affects the contrast and resolution of the image.

As opposed to the Rayleigh scattering, the Compton scattering describes the event in which the photons are scattered by free electrons. When the photons are scattered in this way, they lose a portion of their energy, which can significantly influence the detected radiation spectrum. The amount of lost energy is proportional to the scattering angle - greater scattering angle means that the photon will lose more energy to the electron. The electron which receives the energy from the photon is called the recoil electron. This electron is emitted under the angle corresponding to the direction of the incoming photon. In figure 8, we can see the illustration of the Compton scattering effect.

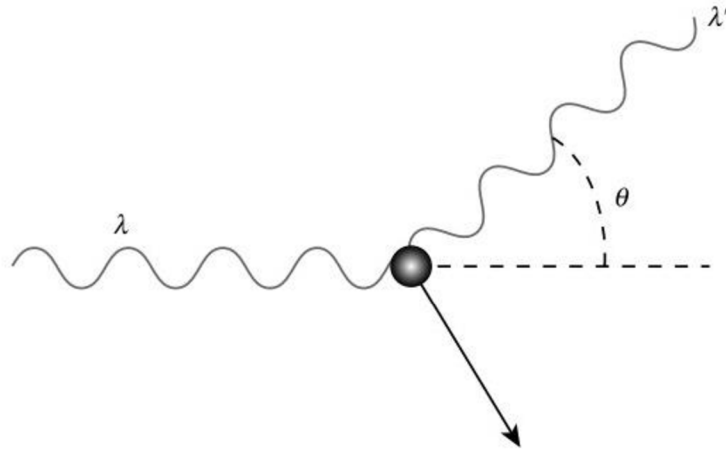


Figure 8 – Illustration of Compton scattering (taken from [2])

The Compton equation (2.2) can be used to describe the change of energy of the photon and its wavelength:

$$\lambda' - \lambda = \frac{h}{m_e c} \cdot (1 - \cos \theta) \quad (2.2)$$

The symbol λ is the wavelength of the photon before scattering, λ' is the wavelength of the photon after scattering, m_e equals to the mass of the electron, θ is the angle under which the photon was scattered, h is the Planck's constant and c is the speed of light. If we substitute the values for m_e , h and c we will obtain a characteristic Compton value ($\frac{h}{m_e c}$) which equals to 2.4 picometers. This equation has several interesting properties – The Compton characteristic wavelength is very small in comparison to wavelengths of x-rays used in medical imaging system (for energy of 10keV, the wavelength equals approximately to 120 pm). This means that the maximum wavelength change is only a small portion of the original wavelength. Another interesting property of this equation is that the maximum value of energy change is only probable for angles near 180 degrees.

2.7 DETECTION OF X-RAYS

For detection of x-ray radiation, we need a material that has an ability to absorb the radiation and an ability to convert the photon energy to an electrical signal. This can be achieved in two ways - directly and indirectly. Essentially, an indirect approach means that the x-ray photons are converted into a visible light spectrum using scintillators. The visible light is then detected by conventional light-sensitive materials. The direct

approach utilizes semiconductor materials, which are able to absorb the photon energy directly and convert it to the electrical signals.

A scintillator is a material, which radiates light when struck by a high energy particle – x-ray photon. In typical x-ray systems, materials such as thallium-doped sodium iodide NaI(Tl) or thallium-doped cesium iodide CsI(Tl) are used for scintillation as they have properties which are the most suitable for this purpose. The most notable problem with the scintillation process is that it is very inefficient, mainly because the visible light after the conversion does not travel in the same direction as the original photons. This means that the visible light photons are emitted in all directions and a very small portion of the signal reaches the subsequent light-sensitive material.

Additionally, the indirect method needs additional photomultiplier to compensate for very low magnitude of the signal. For this purpose photomultiplier tubes are frequently used as they are able to provide high gain, fast response, low noise and they are capable of detecting a single photoelectron. However, all these positive features come with the drawbacks - the devices are very sensitive to outer magnetic fields and are very large. There is an alternative to this method, which uses avalanche photodiodes (APD). Essentially, operation of APD is based on photoelectric effect – it converts the light to electricity. APDs have very large quantum efficiency (QE – incident photon to converted electron ratio) and a wide spectrum response, but they have notably lower gain and produce high amounts of noise. The newest technology is based on silicon photomultipliers. These devices offer gain comparable to photomultiplier tubes and are relatively easy and non-expensive to manufacture. However, they have very high operation requirements as they are very sensitive to fluctuations of voltage and temperature.

The modern direct conversion techniques utilize semiconductors such as amorphous selenium, amorphous silicon, or cadmium zinc telluride (CZT) for the radiation detection. For low energy x-rays, standard silicon is very frequently used as it has good homogeneity and generally, it is a very well stabilized technology. CZT detectors offer the highest possible performance in latest x-ray and γ -ray medical imaging systems, but unfortunately they are very expensive to manufacture. CZT has a very high potential as it has a high atomic number (Cadmium 48, Zinc 30, and Telluride 52) and high density.

CZT also has a wide bandgap, which allows it to be operated at room temperatures. The main disadvantage of this material is that it has poor hole charge transfer properties – this creates polarization problems in high-count systems. Additionally, it is very difficult and expensive to manufacture defect-free CZT crystals.

2.8 ELECTRONICS IN X-RAY IMAGING SYSTEMS

In terms of electronics used for x-ray detection, VLSI (Very Large Scale of Integration) electronics and development of integrated circuits allows to integrate a large number of separate channels into a single silicon chip. Therefore, each imaging pixel of a detector array can be processed by a single electronic channel. This allows the system to have good spatial resolution, dynamic range and also allows post-processing. However, there are a lot of requirements for systems of this complexity – it should be able to amplify and filter signals from each detector element, then perform analog to digital conversion and store the resulting data in digital form. This represents problems such as power limitations, noise production and crosstalk, which require the system to be further improved by additional circuitry.

2.9 COLOR X-RAY IMAGING

Conventional imaging modalities based on x-rays usually rely only on the attenuation data, ignoring the energy of transferred photons. Color x-ray imaging utilizes this energy information and is getting increasing attention in the medical field.

“Color X-ray imaging is already used in some baggage inspection systems, as an automatic exposure control in mammography, and for bone mineral density measurement discrimination of bones and soft tissue using dual-energy contrast-enhanced digital subtraction techniques. VLSI chips that can discriminate against X-ray photon energies are already available in production volumes. The use of a color X-ray in medical X-ray imaging is expected to increase dramatically in the next 5–10 years.”
(Iniewski, 2009, p.18)

X-ray imaging systems are known to have poor ability to detect specific substances in the scanned object. This is due to the fact that these substances are always superimposed to the whole imaged scene. Conventional systems are not able to separate the two signals, however, spectral decomposition could allow us to separate the signal

from the anatomic background and the signal from the contrast substances. In combination with photon counting detectors with reasonable resolution, conventional x-ray imaging modalities should be able to allow selective detection of contrast substances.

The conventional scanners measure attenuation of x-rays, disregarding the energy of photons – the combination of different objects can produce the same attenuation, while the color x-ray systems can distinguish individual objects and even tell us the material they are made of. The main goal of color x-ray imaging is to improve the detectability of detail, to enable us to distinguish different materials and tissues and to enhance the visibility of contrast substances.

3 COMPUTER TOMOGRAPHY

As mentioned earlier, traditional x-ray imaging systems have a number of limitations which make their use very limited. The main problem with these imaging modalities is that the three-dimensional objects are reduced into two-dimensional images. Traditional x-ray images are unable to provide good contrast of soft tissues and require qualified personnel to assess them. The majority of these problems can be solved using a more complex and demanding technology to create a 3D projection using x-rays. Computer tomography uses principles described earlier in this work to take many images of the patient from different angles. Based on these tomographic images, a 3D projection is calculated. CT requires quite a lot of computing power, although in our modern era, this poses no real problem as the conventional PCs already have enough computing power.

3.1 BASIC CT PRINCIPLE

In figure 9, we can see schematic representation of the CT scanning process. The CT scanner makes a large number of measurements of attenuation through the cross section of the body. The system then creates a digital image of the cross section where each pixel of the image represents an average attenuation of a box-like element called a voxel. A pixel is a two dimensional unit – if we take the thickness of the cross section into consideration, we receive the voxel, which is essentially a 3D equivalent of a pixel. Each measurement determines the amount of radiation which was lost while passing through a specific material of a finite thickness. Each of these measurements is called *ray sum* as the measurement of attenuation in one straight line is basically a sum of attenuations of all materials in the way between the detector and the x-ray tube. The individual rays are then collected in sets which we call *projections*. To create a 3D image, we need to make a large number of projections as the voxel must be viewed from several different angles. This generally means that the CT machine makes one projection then rotates by 1 degree, makes next projection and this continues until the whole cross section is scanned.

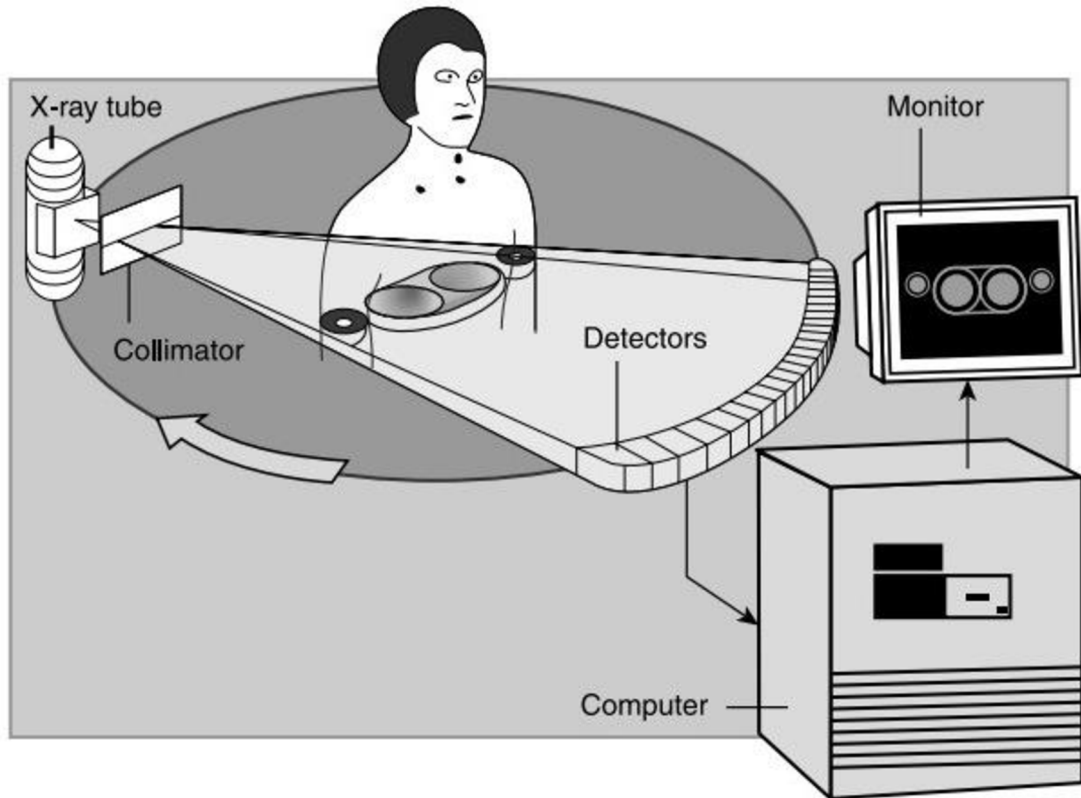


Figure 9 – Illustration of CT scanning process (taken from [2])

There is a quantitative scale to describe the radiodensity for usage with respect to voxels. This scale is called Hounsfield unit (HU) scale or CT numbers. The origin of this scale is the CT number of water which equals to zero, the scale then goes down to -1000 which is the CT number of air and up to 3000 which corresponds to the most attenuating materials. For the material of attenuation coefficient μ , the HU is given by equation 3.1:

$$HU = 1000 \cdot \frac{\mu - \mu_{water}}{\mu_{water} - \mu_{air}} \quad (3.1)$$

Where μ_{water} represents the linear attenuation coefficient of water and μ_{air} represents the linear attenuation coefficient of air. The majority of CT scanners are calibrated with respect to water.

3.2 GENERATIONS OF CT SCANNERS

The concept of Computer Tomography was introduced by Godfrey Hounsfield in 1972. The first CT designs were known as axial transverse scanners (CAT scanners) and these

earliest designs were basically just machines to prove that the concept of three dimensional images is possible. The first generations were practically impossible to use in practice in the past but today, CT scanners made big progress mainly in terms of scanning times, spatial resolution and shorter computer reconstruction and as a result CT is now widely used in medicine.

CT machines are technically very complex and expensive. However, when we omit this construction complexity and price, we can imagine that the CT is basically a set of rotating x-ray tubes and detectors. In figure 10, we can see a schematic picture of a CT imaging system. For 3D reconstruction, a lot of computing power is needed and therefore, each of the detectors has its own internal computer implemented. Aside from medical use, Computer Tomography is widely used in luggage inspection at airports and non-destructive evaluation of materials.

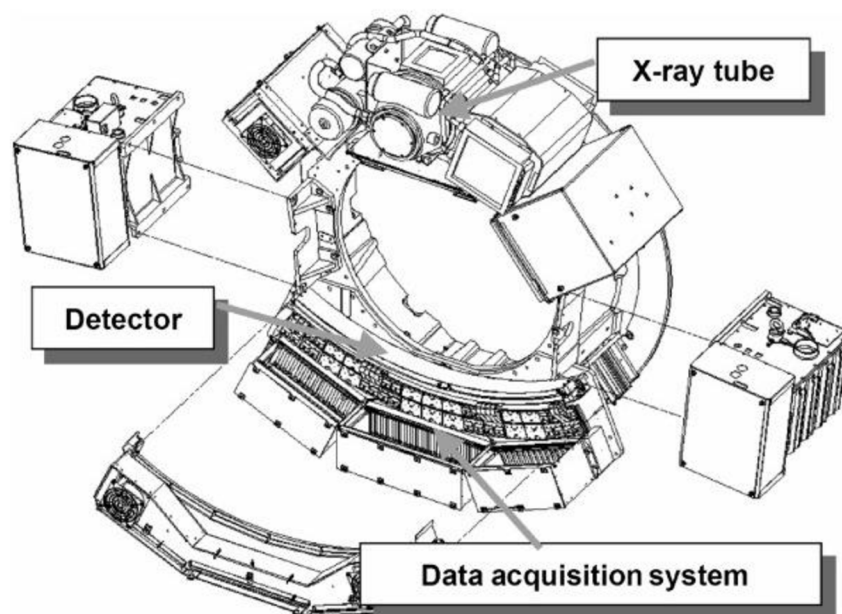


Figure 10 – Illustration of typical CT system (taken from [2])

First generations of CT used one generator of x-rays with one detector. The x-rays therefore travelled in parallel. To scan a cross section, the tube with the detector first had to shift from one side to the other side, then rotate and this process was repeated until the whole cross section was scanned. As a result, the earliest versions required a few minutes for a single scan and due to this they were not applicable to the regions of body where movement could easily occur (f. e. head) as it would most probably result in

unreadable data. The contrast of resulting images was unparalleled at the time but the resolution was very poor and with the combination of very long scan times, this design practically ceased to exist.

The second generation of CT featured a fan beam of x-rays with a set of detectors. This essentially shortened scan times from minutes to seconds as the collimated fan beam enabled to scan bigger area at once. The rest of the construction stayed the same as in the first generation – first, the detectors and x-ray tube had to shift from one side to the other and then they rotated.

The third generation machines eliminated the shifting movement from the scanning system which further improved scan times. The third generation CT system is schematically represented in figure 9. The set of detectors is shaped into the half-circle and the x-ray tube produces fan beam while both parts of the system simultaneously rotate around the patient. Currently, this generation, with various technological improvements and modifications, is the most common among the CT machines. The fourth generation of CT featured detectors around the whole gantry while the x-ray tube was the only part which rotated and the fifth generation replaced x-ray tube with electron gun. However, these generations are not used in practice.

3.3 SLIP RING TECHNOLOGY AND HELICAL SCANNING

One of the most notable technologies used in CT machines is *slip ring technology*, which is used in the sixth generation scanners. The slip ring technology was invented for use in systems which require transmission of power and/or data while maintaining unlimited, continuous rotation. In medical imaging systems, we can find slip rings in CT scanners, MRI scanners, high resolution ultra-sounds and digital mammography systems. In addition, slip rings can be found in various vehicles, helicopters, turbines etc. This technology enables to transmit power and/or data from stationary components to rotational components of the system through connection of conductive brushes, placed on the stationary component, and circular conductors, placed on the rotating component. The brushes are pressed to the circular conductors so the connection is

maintained with no need for any cable. In figure 11, we can see a slip ring in one of CT scanners.

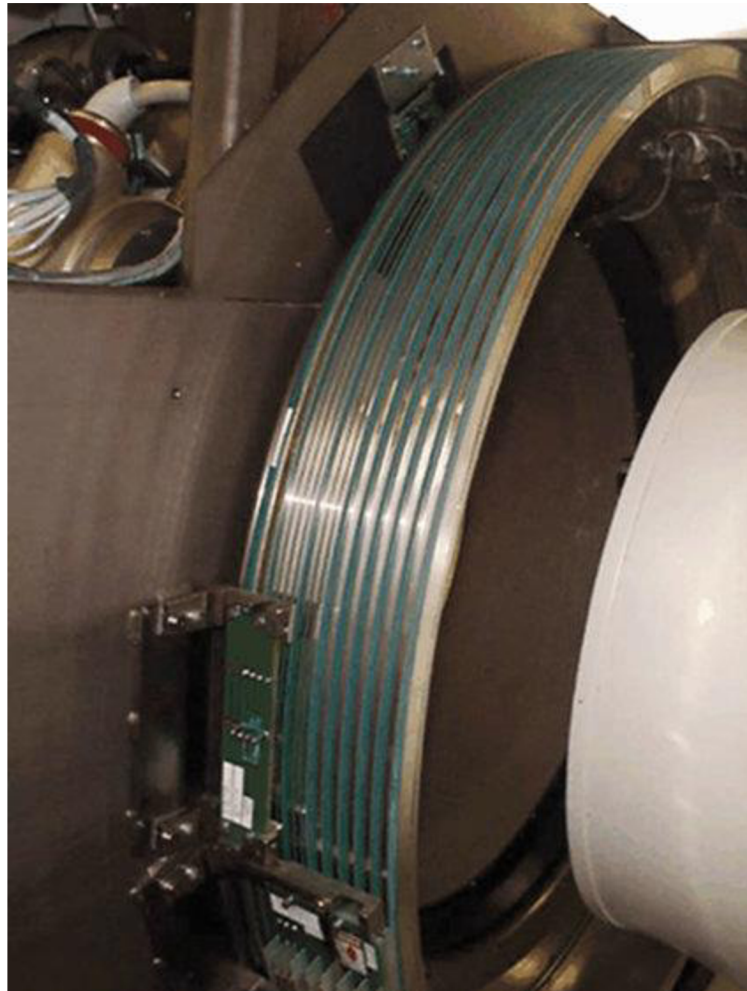


Figure 11 – Slip ring in CT scanner. Retrieved May 17, 2016 from <http://www.wikiradiography.net/page/Slip+Rings>)

In conventional CT scanners, we receive an image for 360 degrees, then the gantry moves on and the next 360 degrees of data is acquired. These scanners are limited by cables through which the data and power are transmitted as the rotating parts are not able to make rotation of more than seven hundred degrees – the system makes scan of one plane and then needs to rotate in the reverse direction to be able to scan next cross section. Due to the slip ring technology, helical CT scanners were invented. These machines cover non-planar geometry – in this method, the table with a patient is slowly moving while the cross section is being scanned. In figure 12, we can see comparison between the conventional CT and helical CT scanners.

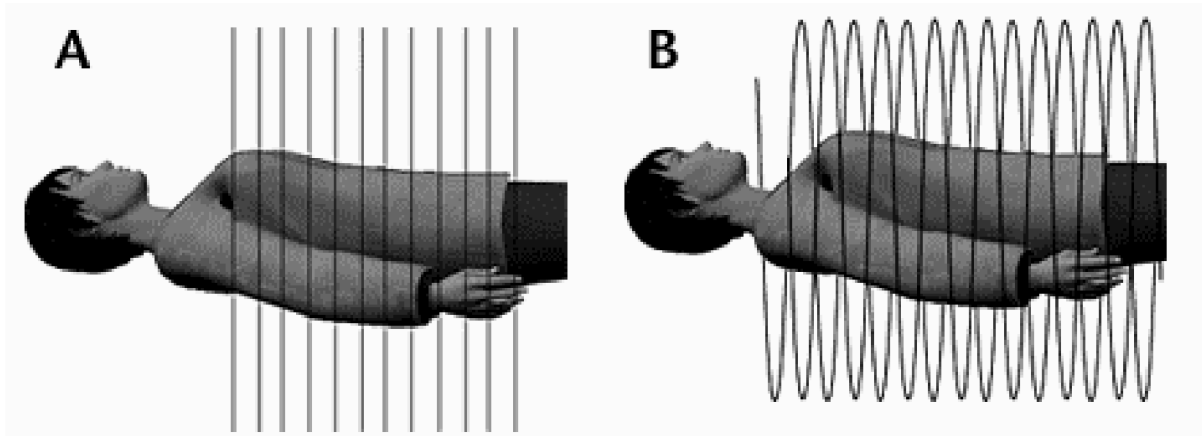


Figure 12 – A) Planar scans of conventional CT system B) Helical scanning. Retrieved May 17, 2016 from <http://imaging.cancer.gov/patientsandproviders/cancerimaging/ctscans>

Spiral scanning introduces a new important value regarding the movement of the patient which is called the pitch factor. The pitch value describes the distance the body is moved during one beam rotation. It can be also described by equation 3.2:

$$HP = \frac{d}{T} \quad (3.2)$$

Where d is the distance per revolution and T is the width of the x-ray beam. The pitch value of 1 or less is typically used. Higher values of the pitch factor lead to shorter scan times and lower radiation doses at the cost of reduced resolution of the image.

The invention of helical scanning was revolutionary as it enabled to take pictures of the body parts where movement presented serious problems (scans of lungs, heart etc.) – shorter acquisition times lead to notably smaller impact of movement artifacts on the image. Another big advantage of helical scanning is that the data acquired are not broken into individual slices – the helical scan produces continual set of data which extends over some volume of the patient’s body. This essentially means that with low pitch values, we can notably decrease the increment in y-axis and therefore, improve the ability to detect small objects and generally improve the image quality.

3.4 MULTI-SLICE CT SYSTEMS

The development of CT scanners is directed towards obtaining as much data as possible in the shortest time intervals possible. The slip ring technology and higher speed of the rotation are one of the directions which were chosen in the development of modern CT

scanners, but this approach has its limits. The gantry is very heavy (around 900kg) and the forces acting on the whole system (especially x-ray tubes) are very harsh. For these reasons, the multi-slice CT scanners were developed.

In multi-slice CTs, additional rows of detectors are used so it is possible to detect multiple cross-sections simultaneously. Modern machines have up to 128 rows of detectors. Additionally, the multi-slice principle can be combined with helical scanning – in this case the formula for pitch factor (3.2) is slightly changed:

$$HP = \frac{d}{N \cdot T} \quad (3.3)$$

Where N represents the number of detector rows. The advantages of such systems are that for one revolution we detect multiple cross sections – this leads to increase of detected volume and improvement in spatial resolution. In addition, the utilization of x-ray beam is improved too. This, however, comes at the cost of *cone beam artifact* as the multiple beams which are detected by additional detectors are not perpendicular to the longitudinal axis of the patient. The cone beam artifact is intensified with the increasing number of detector rows and is also influenced by pitch value. In figure 13, we can see how lower pitch values cause the overlapping of individual cross sections. When reconstructing the data acquired from this system, algorithms which can correct this artifact need to be used.

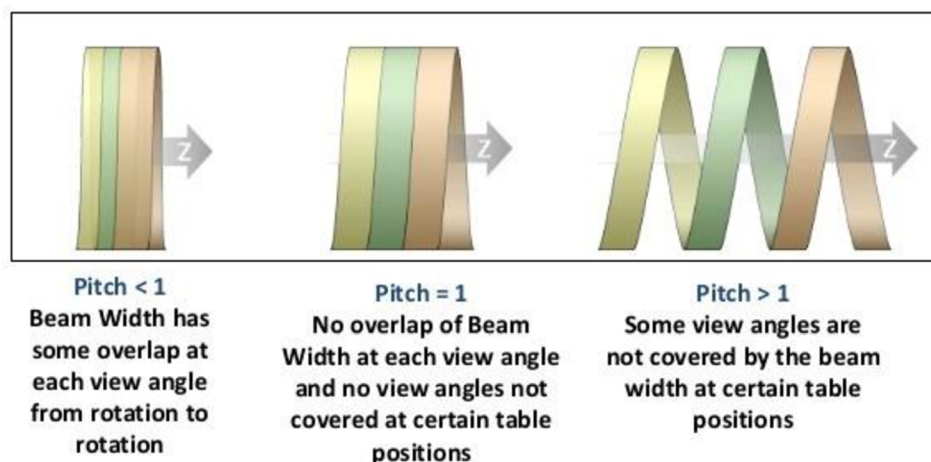


Figure 13 – Illustration of cone beam artifact for different pitch values. Retrieved May 17, 2016 from <http://www.slideshare.net/VivekElangovan1/ctdi-42682868>

4 MAGNETIC RESONANCE IMAGING

Another major topic of my bachelor thesis is dedicated to magnetic resonance imaging (MRI). Magnetic resonance imaging is relatively new imaging technique in medicine and is primarily used in radiology to create functional and anatomical images of the human body. Contrary to x-ray imaging modalities and various other methods, magnetic resonance is considered one of the safest imaging techniques as it does not use ionizing radiation to create images. MRI generates images of soft tissues with excellent quality and thus, it is especially useful in neurological, musculoskeletal, cardiovascular, and oncological imaging.

The images of MRI are primarily generated using signals from hydrogen nuclei of water and fat in human body – more specifically from protons of hydrogen nuclei. The signal acquisition is based on a phenomenon called nuclear magnetic resonance (NMR), which deals with interactions between spins and magnetic moments of protons in nuclei in human body and strong external magnetic fields.

MRI is considered one of the most versatile imaging techniques. The versatility of MRI comes from the fact that it can provide a large number of types of contrast with minimum requirements in terms of equipment altering. The types of contrast include proton density, T1 and T2 relaxation times, magnetic susceptibility and a number of others – the list is continuously expanding as new techniques are being developed. T1 and T2 relaxation times of the human tissues are the most commonly used contrast types in clinical MRI. T1 relaxation time is mainly used to create anatomical images of various organs and tissues of human body, while T2 contrast is used mainly in imaging of pathological tissues like tumors.

4.1 THE HISTORY OF MAGNETIC RESONANCE IMAGING

Nuclear magnetic resonance was discovered in 1938 by Isidor Isaac Rabi (1944 Nobel prize for physics). In 1946, it was further developed as an experimental technique by Felix Bloch and Edward Mills Purcell independently (they shared the Nobel prize for physics in 1952). Since then, NMR was used as a major experimental technique in

chemistry and solid-state physics. In magnetic resonance imaging, the localization of the signal is achieved by applying linear gradients of strong magnetic fields. This technique was discovered in early 1970s by Paul Lauterbur and Peter Mansfield (they shared the Nobel prize for medicine in 2003). First MRI scanners for commercial use became available as early as in the 1980s. Table 1 in the appendix of this work represents a list of the most notable scientists and discoveries regarding the development of magnetic resonance imaging.

4.2 NUCLEAR MAGNETIC RESONANCE

Nuclear magnetic resonance is a phenomenon which represents basis for magnetic resonance imaging techniques. As already mentioned in the previous chapters, NMR is based on interactions between the magnetic moments and external magnetic fields.

The atomic nuclei contain electrically neutral neutrons and positively charged protons - we can say that atomic nuclei are positively charged as a whole. Both neutrons and protons have a physical property called *spin*. Despite being quantum physics property, a spin can be simply described as the spinning motion of a particle around its own axis. The individual spins of all neutrons and protons in one nucleus produce so-called nuclear spin of the whole nucleus. Generally, the nucleus can have either no spin, spin of $\frac{1}{2}$ or spin higher than $\frac{1}{2}$. As expected, we cannot observe the NMR of nuclei with no spin. Table 2 in the appendix presents a list of elements of interest with their spin values.

The nuclei with non-zero spin also have a property called *magnetic moment* – the spinning motion of the electrical charge is similar to the electrical current in a simple closed loop, which possesses a magnetic moment. The nuclear magnetic moment can also be described by formula 4.1:

$$\mu = \gamma \cdot I \cdot \hbar \quad (4.1)$$

Where I is a nuclear spin, \hbar is a Planck's constant divided by 2π and γ is a gyromagnetic ratio, which is a characteristic property of every nucleus. The NMR phenomenon is based on interactions between these magnetic moments and external magnetic fields.

Magnetic resonance imaging relies on signals detected from nuclei (i.e. protons) of hydrogen in water and fat of human body. Therefore, the rest of this chapter will deal only with interactions between protons and external magnetic fields. The interactions can be described via quantum model and classical model.

4.2.1 QUANTUM MODEL - PARALLEL AND ANTIPARALLEL PROTONS

In MRI, the source of signal is an electric current induced in the detection coil by the magnetic moments. The magnetic moment of one single proton is very small and therefore not detectable – the protons in the examined tissue need to produce the detectable signal together. Normally, the protons in human body have a completely random orientation and their respective magnetic moments cancel out, which essentially means that no net magnetic moment is produced. When the proton with the magnetic moment $\vec{\mu}$ is placed in the external magnetic field \vec{B} , the direction of the magnetic moment will attempt to align with the direction of the external magnetic field. This can be likened to the needle of a compass, which aligns itself with the magnetic field of our planet. The large number of protons which co-operate in this way creates a net magnetic moment, which can produce the detectable signal.

In quantum mechanics, the value of spin gives us the number of measurable energy levels (Zeeman energy levels) of a particular nucleus when placed in an external magnetic field. The quantum mechanics also describes that particles cannot change their spin and energy continuously – they can only assume discrete values. With this in mind, we can deduce that the nucleus of hydrogen (spin of $\frac{1}{2}$) has two measurable Zeeman energy levels, which are called E_+ (E parallel) and E_- (E antiparallel). The fraction of either energy states (parallel or antiparallel to the magnetic field) depends on the strength of the external magnetic field and thermal agitation. If we decrease the temperature to the absolute zero, the ratio between parallel and antiparallel protons comes close to the infinite. In other words, the protons will be aligned with the direction of the external magnetic field (parallel state) and in the lower energy state (antiparallel protons have higher energy than parallel ones). At body temperature, a number of parallel and antiparallel protons are nearly equal. However, the parallel fraction of the protons will always be greater by a little amount. If we subtract the number of

antiparallel protons from the number of parallel ones, we receive the number of protons referred to as *spin excess*. The sum of magnetic moments of these protons is called magnetization M .

When the number of excess protons reaches its maximum (and thus when M is at maximum) and is no longer changing, the E+ and E- protons are considered to be at thermal equilibrium. The equation 4.2 says that the magnetization at thermal equilibrium is directly proportional to the strength of the magnetic field (B_0) and to the proton density (N_p), and inversely proportional to the absolute temperature (T).

$$M = c \cdot \frac{B_0 \cdot N_p}{T} \quad (4.2)$$

The c is the constant for proton ($c = \frac{\hbar \cdot \gamma}{2k}$), where k is Boltzmann constant, \hbar is Planck's constant divided by 2π and γ is a gyromagnetic ratio.

4.2.2 CLASSICAL MODEL - PRECESSION MOTION AND LARMOR FREQUENCY

The previous chapter describes how the distribution of protons in two energy states (parallel and antiparallel) create the magnetization vector M . This chapter will deal with change of the orientation of this vector, when a magnetic field is present.

Classical physics describes that if a magnet is placed into a magnetic field, the magnetic field will try to turn the magnet in such a way that the magnetization vector of the magnet aligns with the direction of the magnetic field. The force which turns the magnet is called *torque*. If a torque acts on a spinning object (proton), the spin axis of that object will move in a perpendicular direction to the twisting force of the torque which results in a motion called *precession*. In figure 14, we can see a simplified picture of proton with the magnetic moment $\vec{\mu}$ (on the left) and its precession around the magnetic field \vec{B} (on the right).

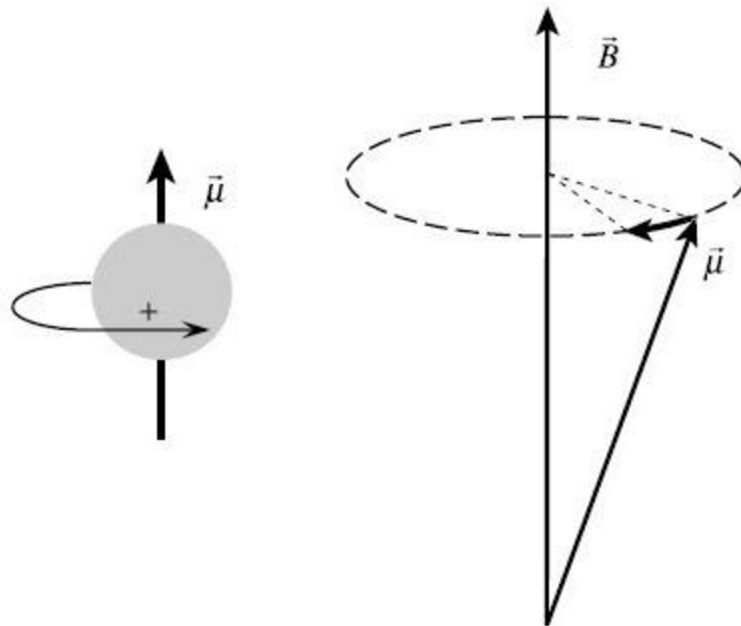


Figure 14 – Precession of a single proton around the magnetic field (taken from [2])

The angular frequency of this motion is described by the Larmor equation (4.3). We can see that the frequency is directly proportional to the strength of the static magnetic field. Values of Larmor frequency for various elements at 1 Tesla are listed in Table 2 in the Appendix.

$$\omega = \gamma \cdot B \quad (4.3)$$

The previous explanation dealt with only one proton, but for MRI to work, we need a large number of protons. When we consider a large number of protons with magnetic moments $\vec{\mu}$, the magnetization vector will be a sum of all individual magnetic moments and it will perform the same motion around the direction of the magnetic field.

4.2.3 QUANTUM MODEL OF MAGNETIC RESONANCE

As already mentioned before, the signal for MRI comes from magnetic moments of protons. This signal is basically an electric current induced in the receiver coil by the magnetization vector M which is a sum of individual magnetic moments.

The direction of magnetization vector must vary in time to induce the current in the coil- the direction of this vector needs to alternately change. At the thermal equilibrium, the vector is not capable to induce any detectable signal as it is parallel to the direction

of a magnetic field which essentially means that for the magnetization vector to induce a current in the coil, we need to disturb the equilibrium between protons in parallel and antiparallel states.

“For as long as the protons are irradiated, a net absorption followed by a net release of energy will occur, and magnetization vector M will flip back and forth between the parallel and antiparallel directions. This exchange of energy between protons and photons is the physical phenomenon called nuclear magnetic resonance.”(Drastich, 2000, p.44)

The thermal equilibrium is not static – the ratio between parallel and antiparallel protons remains constant but individual protons jump back and forth between these two energy states through exchanging the energy between each other. When the system is at equilibrium, the number of changes from parallel to antiparallel state is equal to the opposite changes – adding energy can easily disturb the equilibrium and bring the system to the resonance. This can be achieved by irradiating the protons with electromagnetic radiation in radio-frequency (RF) domain. The RF radiation must fulfill a condition called *resonance condition*, which says that the energy of photons of the RF radiation must be exactly equal to the energy difference between the two (parallel and antiparallel) energy levels of proton. Furthermore, the frequency of this radiation has to be the same as the frequency of precession motion of the proton (for 1 Tesla, this equals to 42.58 MHz).

4.2.4 CLASSICAL MODEL OF MAGNETIC RESONANCE

Chapter 4.2.2 describes that the sum of individual magnetic moments of protons creates the magnetization vector, which precesses around the direction of the magnetic field with Larmor frequency. The angle of the cone of precession will change in time as the protons gain or lose their energy. In other words, the angle between the magnetization vector and the magnetic field vector change in time due to the energy fluctuations of protons. The angle between the magnetization and magnetic field can be manipulated by exposing the protons to the radio waves of the resonance (Larmor) frequency.

To describe the interaction of the radio waves and the proton, we need to define the coordinate system. For the simplicity sake, we will utilize *stationary (laboratory) coordinate system* in which the magnetic field points in the direction of positive z-axis.

As an electromagnetic radiation, the radio waves are composed of oscillating electric and magnetic fields. The magnetization vector M will be affected by the magnetic field of the radio waves B_1 . Radio waves are transmitted into the patient so that the oscillation of B_1 occurs in x-y plane of the coordinate system (perpendicular plane to the magnetic field direction). As a result, the radio wave creates a vector B_1 , which rotates in the x-y plane with the same frequency and direction as the precession of the magnetization M . Chapter 4.2.2 also describes how the magnetic field causes the precession motion of a proton. The magnetic field B_1 also acts on each proton with torque and therefore, it can cause a type of precession of the vector M around B_1 . The angle of rotation produced by B_1 field is called the *RF flip angle* and is described by the equation 4.4:

$$\alpha = \gamma \cdot B_1 \cdot t_p \quad (4.4)$$

Where γ is gyromagnetic ratio and t_p is the time for which the B_1 field was applied – the flip angle can be controlled by the magnitude or duration of B_1 field.

To describe the precession around the B_1 field, we need to use *rotating frame of reference*. This frame looks identical to the laboratory reference frame but in this case the frame is not static - the x-y plane rotates around the y-axis with Larmor frequency. As a result, the magnetization vector M now appears stationary as it rotates around the z-axis with the same frequency as the rest of the frame. Therefore, B_1 will not move in this case and the magnetization vector M will precess around the B_1 in the same way as it precesses around the direction of the static magnetic field. In figure 15, we can see an illustration of a proton precessing around the direction of magnetic field B_0 and simultaneously around the magnetic field of RF pulse B_1 .

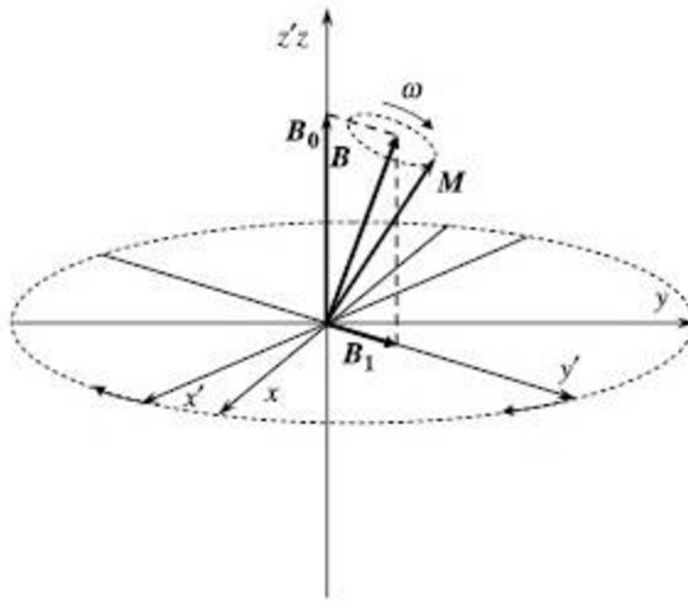


Figure 15 – Simultaneous precession of vector M around the vectors B₀ and B₁ (taken from [2])

4.2.5 FREE INDUCTION DECAY (FID) SIGNAL

If we apply a strong magnetic field to the human tissue, it will induce a magnetic resonance in this tissue and as a result the magnetization vector precessing around the direction of this magnetic field is created. By applying a 90° RF pulse along the transverse plane, we will twist the orientation of the vector M by 90°, which will result in precession of the vector in this transverse plane. If the receiver coil is put close to the examined tissue and is oriented so that its axis is aligned with the transverse plane, the vector M will alternatively point in and out of the coil. As a result, an alternating electric current at the Larmor frequency is induced in the coil – this electric current is called *free induction decay* (FID).

The word *free* refers to the fact that the vector M is precessing freely and is no longer influenced by the RF pulse. The word *decay* represents the fact that this signal is decreasing over time - the particles in the examined tissue will return to the equilibrium from which they were disrupted by the RF pulse. The signal used to reconstruct the image can be FID itself or the so called *echo* of this signal.

4.3 BASIC MEASUREMENT TECHNIQUES

As already mentioned, MRI is a very versatile imaging technique – there are a large number of parameters we can use to create an image and also, there is a lot of measuring techniques. Each of the techniques uses different RF pulses to disturb the thermal equilibrium of magnetization vector M . As a result, the resulting FID signal (or its echo) will show different types of contrast with each measuring technique. These methods include the Saturation-Recovery (SR) technique, Spin-Echo (SE) technique, Inversion-Recovery (IR) technique and several others. Describing all of these techniques goes beyond the scope of this thesis as they are all rather complex processes.

“Generally, the modulation degree in the image will dependent not only on the modulation degree in the scene (tissues) but also on the type of measurement technique (pulse sequence) and selection of the timing of excitations impulses.” (Drastich, 2000, p.55)

The contrast C can be described by relative difference between signal strength of signal a and signal b . Generally, the contrast of an image is given by the formula 4.5:

$$C = \frac{(I_a - I_b)}{I_0} \quad (4.5)$$

Where I_a and I_b are strengths of the signals and I_0 is a scaling factor – the maximum possible strength of the signal. Differences in signal intensity are influenced by several parameters – the density (concentration) of the protons, the behavior of the protons (T1 and T2 relaxation) and the bulk flow of the protons in blood.

4.4 SPATIAL LOCALIZATION

The basis for spatial localization in MRI is the linear relationship between the precession frequency and the strength of the magnetic field, described by the Larmor equation (4.3). This equation essentially says that any spatial dependence of B will result in the same dependence of ω . This spatial dependence of B is generally gained via creating a linear gradient of B . As a result, the field B and frequency ω will become a linear function of position r (4.6 and 4.7). G represents the linear gradient of magnetic field B .

$$B(r) = B_0 + G \cdot r \quad (4.6)$$

$$\omega(r) = \omega_0 + G \cdot r \quad (4.7)$$

The simplest way to create such a gradient is to use two loops of wires with a current flowing in opposite direction through them (figure 16). In real MRI systems, these gradient coils represent very complex systems.

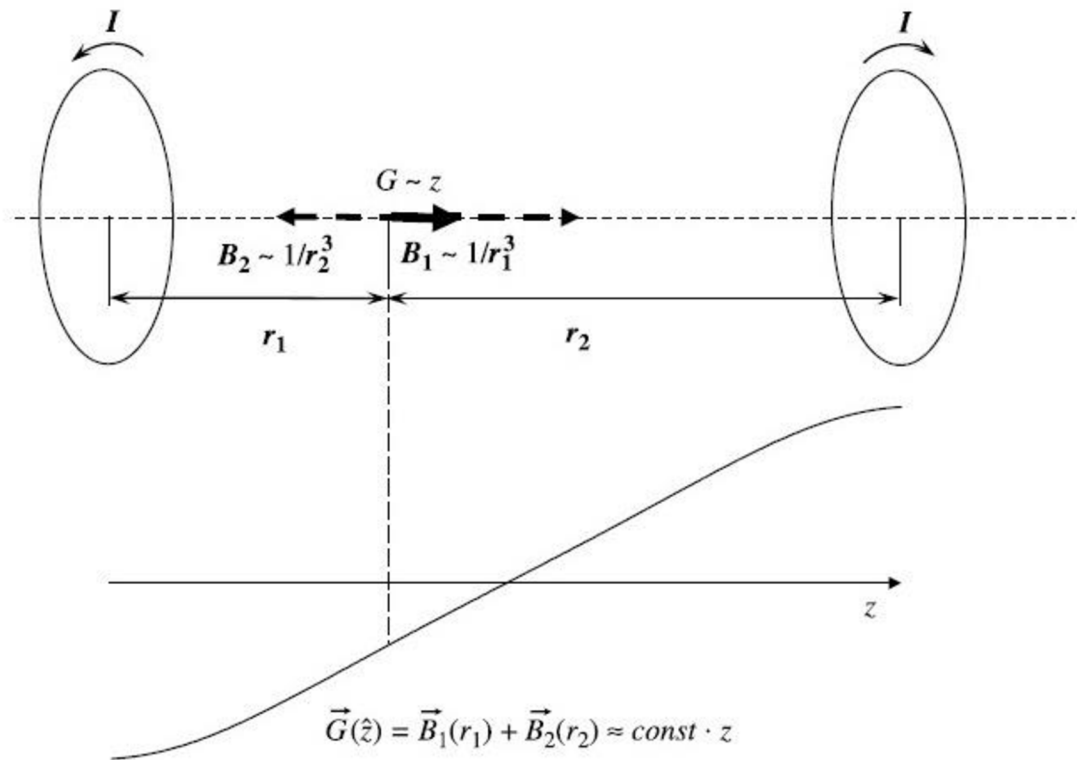


Figure 16 – Pair of gradient coils used for localization on the y-axis (taken from [2])

To create a 3-D image of the scenery, the spatial localization is needed in all three dimensions. This is achieved by selecting the slice in one dimension and then localizing the signal in other two dimensions via frequency and phase encoding methods (figure 17).

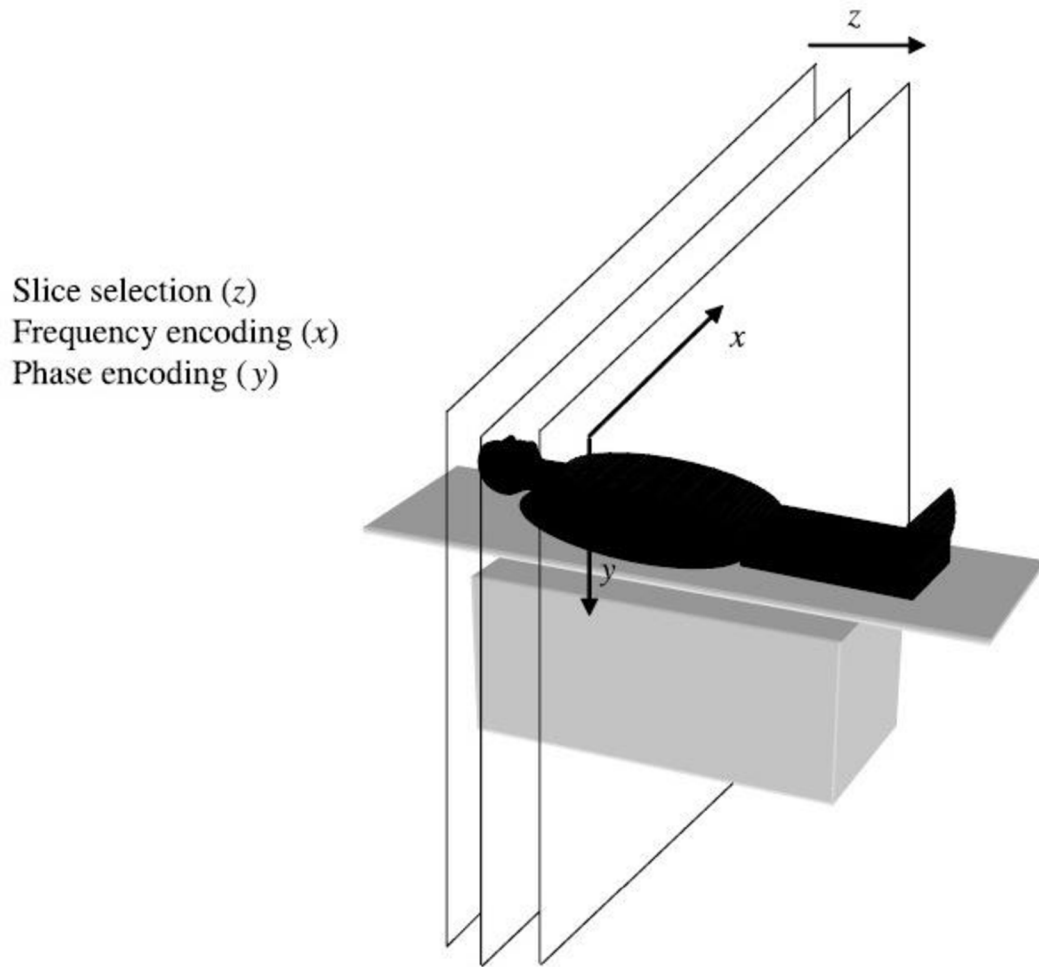


Figure 17 – Individual processes of spatial localization (taken from [2])

4.5 MRI SYSTEM

In figure 18, we can see a typical MRI system configuration. The superconducting magnet is the system's source of the main magnetic field, which polarizes nuclei of atoms in the patient's body. In clinical systems, strength of the field of these magnets range from 1 to 3 Tesla. For experimental purposes, magnets of as much as 7 Tesla are used. The cylindrical gradient coil is placed in the opening, concentrically to the superconducting magnet. It consists of three sets of windings, which generate linear gradient fields in the directions of the coordinate system for spatial localization purposes. The next part is an RF body coil, which produces radio waves to excite the spins in the examined tissue. The receiver coil array is then used to pick the FID signal produced by the pulses and sends the signal to the rest of the system to create the final image.

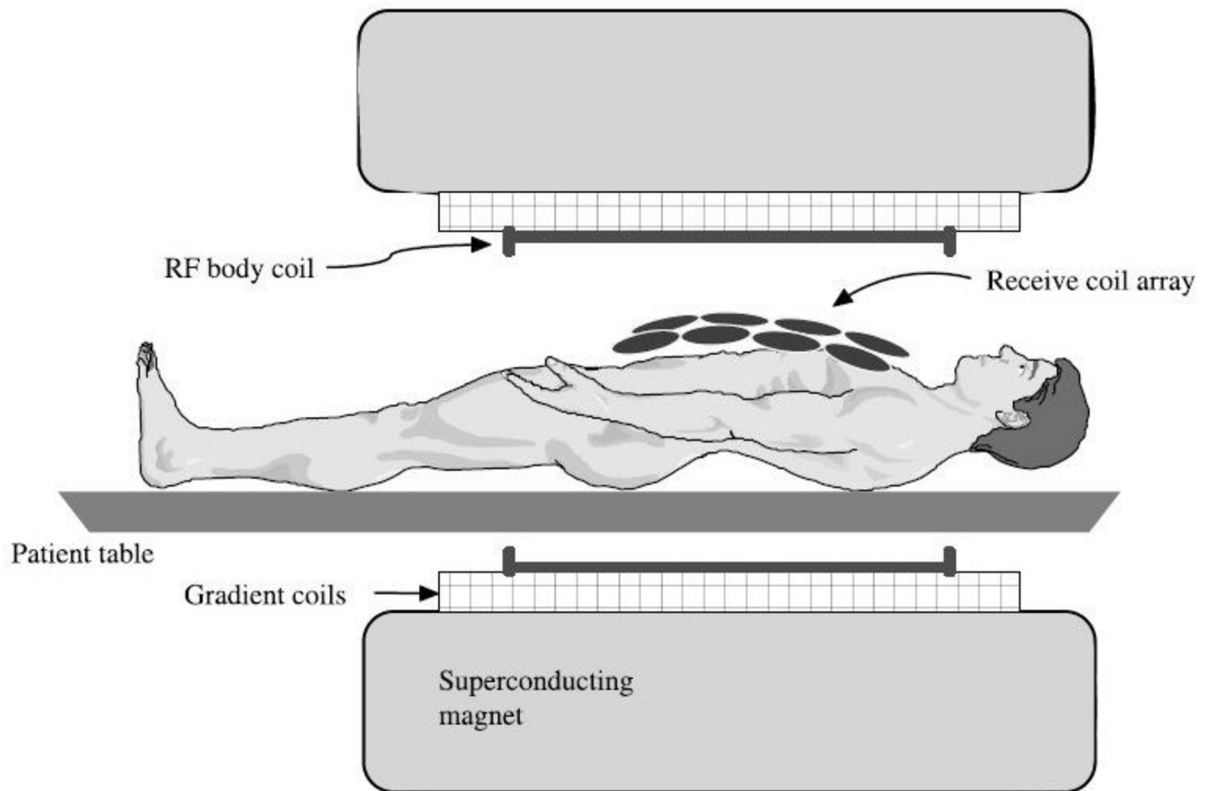


Figure 18 – Typical MRI system configuration (taken from [2])

Each system varies in a large number of different specifications. The magnitude of the magnetic field strength, the quality of gradient and RF coils and the overall quality of parts of the system which are used to compensate for artifacts in the final image determine the quality of the system.

5 CONCLUSION

To conclude my work, I will present a comparison between the individual methods which I described. In the appendix of this thesis, several figures showing the final images provided by individual methods can be found. Additionally, table 3 in the appendix contains comparison between individual properties of available imaging modalities.

While they are based on the same physical phenomena and principles, traditional x-ray imaging and CT scanners are quite different imaging modalities. Traditional x-ray imaging systems are inexpensive to manufacture and have rather low operating cost. However, their usage is limited due to low contrast in case of imaging soft tissues and non-quantitative results which require qualified personnel to assess the data. The CT provides solution to the problems which traditional x-ray systems represent although the drawback of the Computer Tomography is that the machines are basically large industrial machines which are expensive to manufacture and have great operating cost as they require hundreds of kilowatts of power and a lot of space. The operating cost is also a big issue in the case of MRI systems.

The MRI is based on a rather complex physical phenomenon called nuclear magnetic resonance and as opposed to the traditional x-rays and CT, it does not utilize harmful radiation of any kind. Compared to the CT and conventional x-rays, MRI is an imaging method which excels in creating images of soft tissues. However, the MRI is much more demanding on the cooperation of the patient as the procedure of signal acquisition is a lot longer and it is very important to minimize any motion of the patient during the scan. Additionally, MRI presents some contraindications which are rather unique for this method – the patient should not have any implants or prosthesis made from metals, a pacemaker etc. as the strong magnetic field would most probably cause a fatal injury in these cases. The MRI scan is also rather unpleasant experience for claustrophobic patients as it requires them to stay still in a very small space of the MRI system for a long time. MRI is a very versatile technique as it is able to produce a lot of different contrasts - the NMR phenomenon can create a large number of parameters

which can contribute to the final image. X-ray based techniques lack this versatility as the only relevant parameter is the attenuation of x-ray radiation.

The ultrasound imaging is very versatile as well - ultrasound modalities are used for many types of examination. It is also the only modality which is currently manufactured as portable systems. Regarding the nuclear imaging methods like PET and SPECT, they are excellent in imaging the function of various organs as they use special substances to increase the contrast between the structures that we want to see and other tissues. While CT and MRI provide images with respect to the structure of the tissue, the nuclear imaging methods are best suitable to provide images regarding function of the examined areas. Each of these imaging techniques suits for different situations in medical use. For bone fractures, traditional x-ray systems are unlikely to be replaced and for images of a head, the CT is and will be unmatched. The MRI is useful in neurological, musculoskeletal, cardiovascular, and oncological imaging – disciplines in which the CT does not provide optimal results. With this in mind, we can expect that all imaging methods will continue to undergo significant development.

BIBLIOGRAPHY

- [1] DRASTICH, A. *Medical Imaging Systems: X-Ray, Computed Tomography, Magnetic Resonance Imaging*. Brno: University of Technology Brno, 2000
- [2] INIEWSKI, K. *Medical Imaging: Principles, Detectors and Electronics*. New Jersey: John Wiley & Sons, Inc., 2009
- [3] Z.H. CHO, *Foundations of Medical Imaging*. John Wiley & Sons. Inc., 1993
- [4] DRASTICH, A. *Tomografické zobrazovací systémy*. Brno: University of Technology Brno, 2004

APPENDIX

Year	Event	Scientist
1922	First observation of a nuclear spin in a beam of silver atoms	Otto Stern and Walther Gerlach
1938	First observation of NMR in an atomic beam	Isidor Isaac Rabi
1944	Isidor Isaac Rabi receives the Nobel prize for physics	
1945	First observation of NMR in bulk material (resonance effect in paraffin wax) by Purcell and his team	Edward Mills Purcell
1946	First observation of NMR in bulk material by Felix Bloch and his team (electromotive force in the surrounding radiofrequency coil)	Felix Bloch
1949	First NMR experiment (Torrey), discovery of spin echoes (Hahn)	Henry Torrey, Erwin Hahn
1952	Edward Mills Purcell receives the Nobel prize for physics	Edward Mills Purcell
1964	First pulse NMR spectrometer by Ernst and Varian Inc.	Ernst, Anderson
1971	Discovery of higher relaxation times T1 and T2 in tumors	Damadian
1972	First MRI image – discovery of spatial localization of NMR signals	Paul Lauterbur
1972	Development of a method based on NMR to study diffractions in solid materials	Peter Mansfield
1974	Slice selection method developed by Mansfield	
1976	First MRI image of a human body part (finger) acquired in vivo	Mansfield and Maudsley
1991	Richard R. Ernst receives the Nobel prize for chemistry for his contribution in the development of high resolution NMR spectroscopy	Richard R. Ernst
2002	Kurt Wüthrich receives the Nobel prize for chemistry for his development of NMR spectroscopy for studying biological macromolecules	Kurt Wüthrich
2003	Peter Lauterbur and Peter Mansfield receive the Nobel prize for medicine for their discoveries in magnetic resonance imaging	

Table 1 – The history of MRI

Nucleus	Larmor frequency at 1T [MHz]	Spin
¹ H	42.577	1/2
² H	6.536	1
³ H	45.414	1/2
³ He	32.433	1/2
⁷ Li	16.547	3/2
¹³ C	10.705	1/2
¹⁴ N	3.076	1
¹⁵ N	4.315	1/2
¹⁷ O	5.774	5/2
¹⁹ F	40.055	1/2
²³ Na	11.262	3/2
³¹ P	17.235	1/2
³⁵ Cl	4.172	3/2
³⁹ K	1.987	3/2
⁸⁷ Rb	13.932	3/2
¹²⁹ Xe	11.776	1/2
¹³³ Cs	5.584	7/2

Table 2 – Elements of interest for MRI

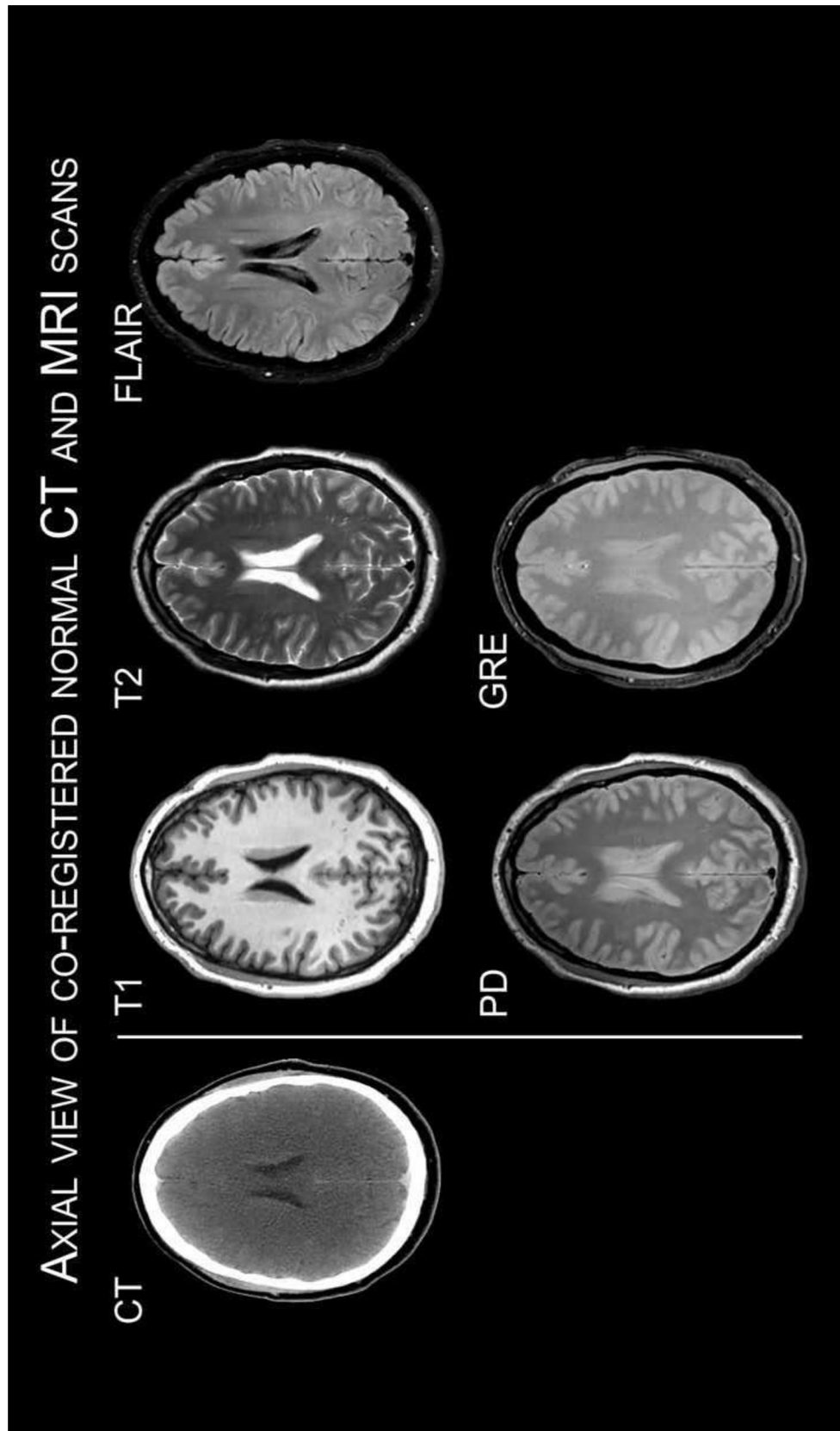


Figure 19 – Comparison between axial view of CT scan and several MRI scans. Retrieved May 3, 2016 from <https://www.youtube.com/watch?v=sz0qd5q6FDU>



Figure 20 – Typical x-ray scan. Retrieved May 3, 2016 from <http://med.fau.edu/research/focus.php>

Imaging type	Ionizing	Image quality	2D/3D	Real-time	Portable	Cost
MRI	No	High	Both	No	No	High
CT	Yes	High	Both	No	No	High
US	No	Medium/high	Both	Yes	Yes	Low
X-ray	Yes	High	2D	Yes	No	Medium
PET / nuclear	Yes	Low	2D	No	No	High /medium

Table 3 – Comparison of individual imaging modalities